

Double-Exchange Model on Triangle Chain

Atsuo Satou

*Department of Applied Physics, Tokyo University of Science,
Kagurazaka 1-3, Shinjuku-ku, Tokyo 162-8601, Japan*

Masanori Yamanaka*

*Department of Physics, College of Science and Technology, Nihon University,
Kanda-Surugadai 1-8, Chiyoda-ku, Tokyo, 101-8308, Japan*

(Dated: November 21, 2018)

We study ground state properties of the double-exchange model on triangle chain in the classical limit on t_{2g} spins. The ground state is determined by a competition among the kinetic energy of the e_g electron, the antiferromagnetic exchange energy between the t_{2g} spins, and frustration due to a geometric structure of the lattice. The phase diagrams are obtained numerically for two kinds of the models which differ only in the transfer integral being real or complex. The properties of the states are understood from the viewpoint of the spin-induced Peierls instability. The results suggest the existence of a chiral glass phase which is characterized by a local spin chirality and a continuous degeneracy.

PACS numbers: 75.10.-b, 75.30.Et, 75.30.Mb, 11.15.-q

I. INTRODUCTION

The double-exchange mechanism [1] has received a special attention as one of the canonical mechanisms which explain the magnetism and transport properties of a class of transition metals. The Hamiltonian which describes it is known as the double-exchange model [2, 3]. Assuming a two sub-lattice structure, de Gennes obtained the phase diagram as a function of temperature and hole concentration, x [3]. The ground state exhibits the antiferromagnetic (AF), ferromagnetic, and canted AF phases [3, 4]. The disordered, two sub-lattice, and helical spin structures and their degeneracies were discussed [3] combining the two sub-lattice structure. These rich structures are induced from competition between the kinetic energy of the e_g electron and the direct AF coupling between t_{2g} spins [3, 5, 6].

On the other hand, studies without imposing the restriction to the two sub-lattice structure have been reported. These results suggest the existence of the ground state without the translation invariance. An existence of the phase separation was reported [4, 9, 10, 11, 12]. (For the model without the direct exchange between t_{2g} spins see refs. [13, 14, 15, 16, 17, 18, 19, 20, 21].) The analysis based on the spin-induced Peierls instability [22, 23] suggest the existence of a super-cell structure of the localized spins. The spin state is distorted with a period which is commensurate with the Fermi momentum so as to open the Peierls gap, thus stabilizing the system. This is isomorphic to the Peierls instability [24]. The only difference is that the spin degree of freedom is distorted, instead of the lattice degree of freedom.

In two or more dimensions, the degree of the phase fac-

tor in the transfer integral plays an important role [25, 26]. For example, the generalized Peierls instability [27] is expected to work and the ground state exhibits a quantum Hall effect [22] if the state satisfies conditions [28]. (See also ref [29].) Actually the staggered π -flux state is stabilized at half-filling in the two dimensional square lattice [22, 30]. The anomalous Hall effect induced from the Berry phase was investigated [29, 31, 32]. The extensive investigations for the phase diagram were performed in two or three dimensions [33, 34, 35] and a flux state with super-cell structure was found away from half-filling.

Recently the most intriguing is the study within the framework of Tsallis nonextensive statistics [36, 37, 38].

In this paper, we study the double-exchange model on the triangle chain to investigate the effects of (i) the phase factor in the transfer integral and (ii) the frustration due to the geometric structure of the lattice. The triangle chain is constructed from the one-dimensional array of the triangles. (See Fig.1.) The triangle is the smallest unit for making a closed loop which is responsible for a non-vanishing flux up to the local gauge transformation. Then, the triangle chain has the simplest lattice structure to study the effect of the phase factor. On the other hand, the geometric structure induces a frustration. The ground state is determined by the competition among the kinetic energy of the e_g electron, the antiferromagnetic exchange energy of the t_{2g} spins, and the frustration. We numerically obtain the phase diagram assuming the ab-

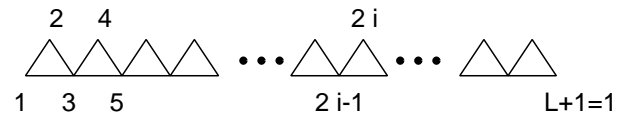


FIG. 1: Lattice structure of triangle chain.

*Electronic address: yamanaka@phys.cst.nihon-u.ac.jp

sence of the phase separation. The ground state exhibits an insulator with a super-cell structure of the t_{2g} spins for a wide range of the parameter space. The state has a continuous degeneracy which is a hallmark of the double-exchange model in one dimension. The spin structure is characterized by an incommensurate spin configuration [39] and a local spin chirality. The spin chirality induces a non-vanishing flux to the e_g electrons. This is an interesting example of the finite spin chirality induced in electronic models without any assistance of other effects, such as the anisotropy in spin space, spin-orbit coupling, lattice distortion, and external magnetic field, etc.. [40]

II. HAMILTONIAN

The double-exchange model on the triangle chain is defined by

$$H = - \left(\sum_{i=1}^L t_{i,i+1}^\mu c_i^\dagger c_{i+1} + \sum_{i=1}^{L/2} t_{2i-1,2i+1}^\mu c_{2i-1}^\dagger c_{2i+1} + h.c. \right) + J \sum_{\langle i,j \rangle} \vec{S}_i \cdot \vec{S}_j,$$

where $c_{i,\sigma}$ is the annihilation operator of the e_g electron at the site i , and \vec{S}_i are localized (t_{2g}) spins which are treated as classical vectors directed along (θ_i, ϕ_i) in the spherical coordinates. We denote the spin configuration by a set $\{\theta_i, \phi_i\}$ ($i = 1, 2, \dots, L$). Moreover, J (≥ 0) is the direct exchange coupling strength between t_{2g} spins. L (even) is the total number of the sites. The number of the triangle is $L/2$. In order to see the effect of the phase factor in the transfer integral, we study two kinds of the model. Their transfer integrals are given by [7, 41, 42]

$$\begin{aligned} t_{i,j}^{\mu=C} &\equiv z_{i,j} = \cos \frac{\theta_i}{2} \cos \frac{\theta_j}{2} + e^{-i(\phi_i - \phi_j)} \sin \frac{\theta_i}{2} \sin \frac{\theta_j}{2} \\ t_{i,j}^{\mu=R} &\equiv |z_{i,j}| = \cos \frac{\Theta_{ij}}{2} \end{aligned} \quad (3)$$

for C- and R-models, respectively. Here Θ_{ij} is the relative angle between the spins, \vec{S}_i and \vec{S}_j . We impose the periodic boundary condition for the e_g electron, $c_{L+1} = c_1$.

For a given spin configuration, $\{\theta_i, \phi_i\}$ ($i = 1, 2, \dots, L$), the transfer integrals, $\{t_{ij}^\mu\}$, are uniquely determined through (2) or (3). When we change the spin configuration, $\{\theta_i, \phi_i\}$, the range of $\{t_{ij}^\mu\}$ forms a set $\{\{t_{ij}^\mu\}\}$. We study the difference of the ranges between $\{t_{ij}^C\}$ and $\{t_{ij}^R\}$, for the same domain, $\{\{\theta_i, \phi_i\} | 0 \leq \theta_i \leq \pi, 0 \leq \phi_i < 2\pi, i = 1, 2, \dots, L\}$, or, in other words, the difference between the sets $\{\{t_{ij}^C\}\}$ and $\{\{t_{ij}^R\}\}$. For a system with two sites, the parameter space, $t_{1,2}^C = z_{1,2}$, contains that of $t_{1,2}^R = |z_{1,2}|$, i.e. $\{t_{1,2}^C\} \supset \{t_{1,2}^R\}$. This is because $t_{1,2}^C = z_{1,2} = |z_{1,2}|e^{i\Phi}$, $\Phi = \arg[\tan(\Im z_{1,2}/\Re z_{1,2})]$, and we can set $\Phi \equiv 0$ without loss of generality. *However, for any lattice (except for tree) the transfer integrals (2) and (3) have the mutually exclusive parameter ranges,*

i.e. $\{\{t_{ij}^C\}\} \cap \{\{t_{ij}^R\}\}^c \neq \emptyset$ and $\{\{t_{ij}^C\}\}^c \cap \{\{t_{ij}^R\}\} \neq \emptyset$, where A^c is the complement of the set A . (See Fig.2(a).) The latter, $\{\{t_{ij}^C\}\}^c \cap \{\{t_{ij}^R\}\} \neq \emptyset$, is not obvious. (This holds even for the simple one dimensional chain with a periodic boundary condition in a finite system size. The effect can be attributed to the boundary condition by a local gauge transformation and becomes unphysical in the thermodynamic limit.) We show that there exist at least two examples in $\{\{t_{ij}^C\}\}^c \cap \{\{t_{ij}^R\}\}$ for the model on a triangle lattice. *This holds for any lattice except for tree.* The first example is

$$t_{1,2}^R = t_{2,3}^R = t_{3,1}^R = \cos \frac{\Theta}{2}. \quad (4)$$

We set the relative angles, Θ , small and the same for simplicity. (See Fig.2(b) for the corresponding t_{2g} spin configuration.) We show that $\{\{t_{ij}^C\}\}$ do not contain (4) as a subset for any value of $(\theta_1, \phi_1, \theta_2, \phi_2, \theta_3, \phi_3)$. *Proof:* We can set $(\theta_3, \phi_3) = (0, 0)$ without loss of generality and get $t_{2,3}^C = t_{3,1}^C = \cos(\Theta/2)$ by setting $(\theta_1, \phi_1, \theta_2, \phi_2) = (\Theta, \phi_1, \Theta, \phi_2)$. The rest parameter can be written by $t_{1,2}^C = \cos(\Theta/2) \cos(\Theta/2) + e^{-i(\phi_1 - \phi_2)} \sin(\Theta/2) \sin(\Theta/2)$, which never becomes $\cos(\Theta/2)$ for $\phi_1 - \phi_2 = 0$. Because, in order to make $t_{1,2}^C$ real, we have to set $\phi_1 - \phi_2 = n\pi$ (n =integer) which inevitably leads to $t_{1,2}^C = 1$ or $\cos \Theta$. This contradicts (4). \square

One might consider that this property is due to a finite Peierls phase along the path $1 \rightarrow 2 \rightarrow 3 \rightarrow 1$, because the solid angle among \vec{S}_1 , \vec{S}_2 , and \vec{S}_3 is equivalent to the magnitude of the flux penetrating the triangle. However, this naive observation fails. Even when the three spins are coplanar, there exist an element in $\{\{t_{ij}^C\}\}^c \cap \{\{t_{ij}^R\}\}$. The second example is

$$t_{1,2}^R = \cos \frac{\Theta_{1,2}}{2}, \quad t_{2,3}^R = \cos \frac{\Theta_{2,3}}{2}, \quad t_{3,1}^R = \cos \frac{\Theta_{3,1}}{2}, \quad (5)$$

with the restrictions $\Theta_{1,2} + \Theta_{2,3} + \Theta_{3,1} = 2\pi$ and $t_{i,j}^R > 0$. (See Fig. 2(c).) We show that $\{\{t_{ij}^C\}\}$ do not contain the set (5) as a subset for any value of $(\theta_1, \phi_1, \theta_2, \phi_2, \theta_3, \phi_3)$. *Proof:* We set $(\theta_3, \phi_3) = (0, 0)$ without loss of generality

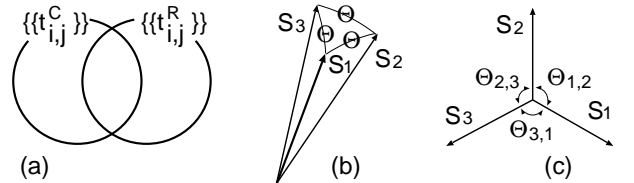


FIG. 2: (a) The relation between sets, $\{\{t_{ij}^C\}\}$ and $\{\{t_{ij}^R\}\}$. (b), (c) Examples of t_{2g} spin configuration which realize the elements in $\{\{t_{ij}^C\}\}^c \cap \{\{t_{ij}^R\}\}$. (b) The e_g electron gets complex transfer integrals by a motion $1 \rightarrow 2 \rightarrow 3 \rightarrow 1$ and (c) it gets real transfer integrals by the same motion. The three spins are coplanar in (c).

and get

$$\begin{aligned} t_{2,3}^C &= \cos \Theta_{2,3}/2 = \cos \theta_2/2 > 0, \\ t_{3,1}^C &= \cos \Theta_{3,1}/2 = \cos \theta_1/2 > 0, \\ t_{1,2}^C &= -\cos \Theta_{1,2}/2 < 0. \end{aligned} \quad (6)$$

This means that the one of the three transfer integrals in $\{t_{i,j}^C\}$ should be negative. \square The general proof is not easy.

III. METHOD

To obtain the ground state we employ the method used in ref. [23]. When we assume an occurrence of the $2k_F$ Peierls instability, the unit cell for the transfer integral contains $2q$ sites (or, in other words, q triangles) at the filling $x = p/2q$ where p and q are mutually prime. The kinetic part in the Hamiltonian (1) is reduced to

$$\begin{aligned} H_t &= - \sum_{j=1}^{L/2q} \left(\sum_{i=1}^{2q} t_{i,i+1} c_{Nj+i-1}^\dagger c_{Nj+i} \right. \\ &\quad \left. + \sum_{i=1}^{2q/2} t_{2i-1,2i+1} c_{Nj+2i-1}^\dagger c_{Nj+2i+1} + h.c. \right), \end{aligned} \quad (7)$$

where $2q$ is the number of sites contained in the unit cell and L is assumed to be the multiple of $2q$. To obtain the ground state, we numerically optimize the functional

$$\begin{aligned} E(\{\theta_i, \phi_i\}) &= E_t(\{\theta_i, \phi_i\}) \\ &+ JS^2 \sum_{\langle i,j \rangle}^{2q} [\cos \theta_i \cos \theta_j + \sin \theta_i \sin \theta_j \cos(\phi_i - \phi_j)] \end{aligned} \quad (8)$$

where $E_t(\{\theta_i, \phi_i\})$ is obtained by the numerical diagonalization of (7).

In the calculation, the $2k_F$ spin-induced Peierls instability for the e_g electron is assumed. For a sufficient large $JS^2 (\gtrsim 0.5)$ and $x = 0.5, 0.25$, we confirmed that the assumption is valid in the following sense: We calculated the ground state energy for a more large super-cell structure which is not characterized by $2k_F$ modulation of the transfer integral and found that the energy is the same upto 10 digits as that of the $2k_F$, and the spacial periodicity is just the repetition of that of the $2k_F$.

IV. PHASE DIAGRAM FOR C-MODEL

We show the phase diagram for C-model in Fig.3(a). The phases are classified by the spin configuration, the modulation of the transfer integrals, and the position of the Fermi point.

A. Several limits

- (1) For $J = 0$ the spin configuration is expected to be ferromagnetic, because the double-exchange mechanism widens the energy band width of e_g electrons to gain the kinetic energy. The ground state is metallic.
- (2) For $J = \infty$ or $x = 0, 1$, the spin configuration exhibits mutually 120-degree structure because of the frustration.
- (3) For $x = 1/2$, in this model the Wigner-Sites cell contains two sites and the state is a band insulator.

B. Region $JS^2 \sim 0$

We have two phases.

- (1) For $x < 0.5$, the state is the ferromagnetic metal (FM). The spin configuration is ferromagnetic and the amplitude of the transfer integrals becomes uniform. The unit cell of the transfer integral coincides with that of the Wigner-Sites cell. Then we have an empty upper band and a partially filled lower band.
- (2) For $x > 0.5$, the state exhibits an incommensurate [39] band insulator (BI-1). For $x = p/2q$, a ferromagnetic $2q$ -merization occurs. The spin configuration is completely ferromagnetic within the domain and incommensurate in long distance. All the energy bands are dispersive. The energy gap opens at the Fermi point.

C. Region $JS^2 \rightarrow \infty$

The spin configuration is nearly 120 degree structure and three spins in a triangle are coplanar.

- (1) For $x < 0.5$, the state exhibits the incommensurate band insulator (BI-2). All the sub-bands are dispersive. (This is in contrast to the simple one dimensional chain where all the sub-bands are dispersionless [23].)
- (2) For $x > 0.5$, the state is in the metallic phase (120M-1). The amplitude of the transfer integral is uniform as a unit of the Wigner-Sites cell and we have two dispersive energy bands.

D. Region $JS^2 \sim 0.25$

The spin configuration has a rich structure because of the competition between the antiferromagnetic exchange coupling and the kinetic energy of the e_g electrons which favors the ferromagnetic spin configuration. The incommensurate insulator with dispersionless energy bands (BI-3) occupies a large region in the center of the diagram. Except for $x = 1/2$, the spin configuration and the transfer integral are incommensurate. (The property is the same that of the incommensurate gapful phase in the simple one dimensional chain [23].) In the masked region in the diagram, the three spins in each triangle are not coplanar. This phase is characterized by a finite

spin chirality and the non-vanishing flux when e_g electron moves around one of the triangles. (The chirality is defined by $\sum_j \langle \vec{S}_1 \cdot (\vec{S}_2 \times \vec{S}_3) \rangle_j$, where j is the index of the triangle.) The state exhibits continuous infinite degeneracy. Therefore, the state is a chiral glass. Each degenerate ground state has a finite chirality. Because of the lattice structure, where the adjacent two triangles share only one site, the degenerate ground states with different magnitude of the chirality are continuously connected to each other. The continuous symmetry breaking is forbidden in one dimension. Therefore, in general, the chirality vanishes because the ground state is a superpo-

sition of the states with different chiralities.

V. PHASE DIAGRAM FOR R-MODEL

The phase diagram for R-model is shown in Fig.3(b).

A. Region $JS^2 \sim 0$

We have three phases.

- (1) ferromagnetic metal phase (FM) for $x < 0.5$,
- (2) incommensurate insulating phase (BI-4) for $0.5 < x < 0.85$, and
- (3) metallic antiferromagnetic phase (AFM) for $0.85 < x$.

In BI-4 phase three spins in each triangle are coplanar within a numerical error. This property is different from that of BI-1 phase in C-model. The AFM phase is sublattice AF and the transfer integrals between the sublattices terminate. Then we have one cosine band and a decoupled dispersionless energy band.

B. Region $JS^2 \rightarrow \infty$

The spin configuration is nearly 120 degree structure and three spins in each triangle are coplanar. There are three phases:

- (1) metallic phase (120M-2) for $0.15 < x < 0.35$,
- (2) incommensurate insulator for $0 < x < 0.15$ (BI-5) and $0.35 < x < 0.85$ (BI-6), and
- (3) incommensurate insulator with dispersionless energy band (BI-7) for $0.85 < x$.

The difference between 120M-1 and 120M-2 phases is as following: The transfer integrals are able to be negative in 120M-1 whereas all the transfer integrals in 120M-2 are positive. The case holds between BI-5, 6, and BI-2 phases. We could not find the difference between BI-5 and 6 phases. In BI-7 the spin configuration and the transfer integral are incommensurate. In this phase all energy bands are dispersionless because some transfer integrals vanish due to the spin configuration

C. Region $JS^2 \sim 0.25$

The incommensurate insulator with dispersionless energy band (BI-8) occupies large region in the center of the diagram except for $x = 1/2$. The transfer integral exhibits a modulation. The masked region is the chiral glass phase. (In the R-model, the transfer integral is replaced by its absolute value so the e_g electron do not be affected by the phase factor.) In the vicinity of full filling, there are several phase boundaries of five phases, BI-4,6,7,8 and AFM. In low dope region, we have four phases, BI-5,6,8 and 120M-2.

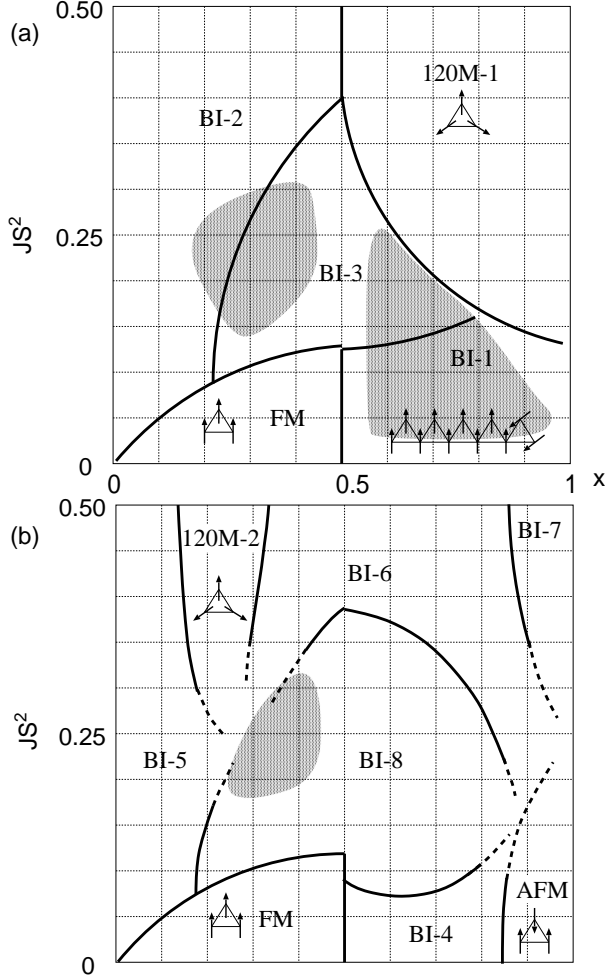


FIG. 3: Possible phase diagrams for C-model (a) and R-model (b) as a function of the electron concentration x and antiferromagnetic direct exchange coupling JS^2 between t_{2g} spins. FM is the ferromagnetic metal phase. BI's are the incommensurate band insulators with incommensurate ferromagnetic polymerization (BI-1), with incommensurate spin (BI-2,4,5,6), and with dispersionless energy band (BI-3,7). 120M-1 and 2 are the metallic phases with nearly 120 degree structure. AFM is the sub-lattice antiferromagnetic phase. The masked regions are the chiral glass phases. The calculation is performed at points where broken lines cross.

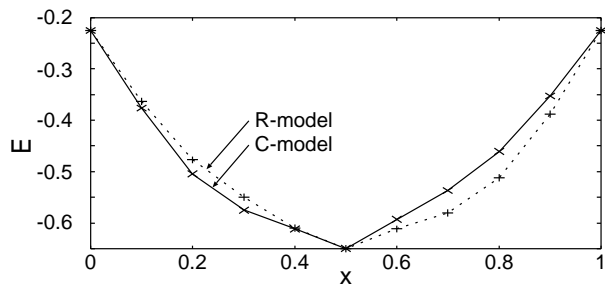


FIG. 4: Estimates of the ground state energy for C-model (solid line) and R-model (broken line) as a function of electron concentration x at $JS^2 = 0.3$. The error bars are smaller than the plotted points.

VI. DISCUSSION

We have obtained a possible phase diagram of the double-exchange model on the triangle chain at zero temperature. The ground state has a rich structure, which includes a band insulator with an incommensurate spin structure [39] and a chiral glass phase. These states exhibit the continuous degeneracy. One of the origins of the degeneracy is due to the structure of the lattice where the adjacent triangles share only one site. The phase diagram is different from the simple one dimensional chain mainly in the following two points: (i) The structure of the phase diagrams of C- and R-models is different. (In the simple one dimensional chain, it is the same.) This is due to the enclosure relation between $\{\{t_{ij}^C\}\}$ and $\{\{t_{ij}^R\}\}$. The transfer integral of BI-2 belongs to $\{\{t_{ij}^C\}\} \cap \{\{t_{ij}^R\}\}^c$, those of BI-7 and BI-6 ($x > 0.5$) belong to $\{\{t_{ij}^C\}\}^c \cap \{\{t_{ij}^R\}\}$, and those of FM and the states at $x = 0.5$ belong to $\{\{t_{ij}^C\}\} \cap \{\{t_{ij}^R\}\}$. Reflecting this property, the different ground states are stabilized in R- and C-models in the same parameter in (x, J) space. For a sufficient large JS^2 , it is found that the ground state energy of C-model is lower than that of R-model

for $x < 0.5$ and vice versa for $x > 0.5$. The example is shown in Fig.4. (Within our analysis, the energy dependence as a function of the electron concentration is concave near $x \sim 0$ and 1. This suggests the absence of the phase separation. However, we need further investigation for the definite result.) Then we may be careful when we substitute or approximate (2) by (3). (ii) For a small J , the global structure of the phase diagram is similar to that of the simple one dimensional chain. However, when J is large enough, the 120-degree structure is dominant because of the frustration. Thus the AF phase which is appeared in the simple one dimensional chain vanishes.

We use the numerical optimization method to obtain the ground state energy. In general, the method is known to be difficult to the function with many variables. We have two sites in the unit cell and two parameters, $\{\theta, \phi\}$, for each site. Therefore, we have $4q$ independent parameters which should be optimized for an electron concentration $x = p/q$. The inverse of the denominator is the resolution of the electron concentration in the phase diagram. Actually, for $x = 1/10$ we have 40 parameters and the number of parameter is a realistic limit of our numerical calculation. We cannot examine the electron concentration with more large denominator by the present method. The connectivity of the critical lines and the precise position of the phase boundaries are not clear due to the above difficulty. The simple extension of the method for many parameters seems not to be realistic.

Acknowledgments

The computation in this work has been done using the facilities of the Supercomputer Center, Institute for Solid State Physics, University of Tokyo and Yukawa Institute for Theoretical Physics. This work is supported by Research Grant for Assistants (and Young Researchers) of Nihon University Research Grant for 2002.

-
- [1] C. Zener, Phys. Rev. **82**, 403 (1951).
 - [2] P.W. Anderson and H. Hasegawa: Phys. Rev. **100**, 675 (1955).
 - [3] P.-G. de Gennes, Phys. Rev. **118**, 141 (1960).
 - [4] É.L. Nagaev, Soviet Phys. JETP, **30**, 693 (1970).
 - [5] D.I. Golosov, M.R. Norman, and K. Levin, Phys. Rev. **B58** 8617 (1998).
 - [6] J.L. Alonso, L.A. Fernández, F. Guinea, V. Laliena, and V. Martín-Mayor, Phys. Rev. **B63** 054411 (2001).
 - [7] É.L. Nagaev, *Physics of Magnetic Semiconductors* Moscow, Mir Publ., 1979.
 - [8] É.L. Nagaev, Sov. Phys.-Uspekhi **166** 833 (1996).
 - [9] S. Yunoki and A. Moreo, Phys. Rev. **B58** 6403 (1998).
 - [10] M.Yu. Kagan, D.I. Khomskii, and M. Mostovoy, Eur. Phys. J. **B12** 217 (1999).
 - [11] D.I. Khomskii, cond-mat/9909349.
 - [12] D.I. Golosov, J. Appl. Phys. **91** 7508 (2002).
 - [13] É.L. Nagaev, Physica **B230-232**, 816 (1997).
 - [14] J. Riera, K. Hallberg and E. Dagotto, Phys. Rev. Lett. **79**, 713 (1997).
 - [15] D.P. Arovas and F. Guinea Phys. Rev. **B58**, 9150 (1998).
 - [16] S. Yunoki, J. Hu, A.L. Malvezzi, A. Moreo, N. Furukawa, and E. Dagotto, Phys. Rev. Lett. **80**, 845 (1998).
 - [17] E. Dagotto, S. Yunoki, A.L. Malvezzi, A. Moreo, J. Hu, S. Capponi, D. Poilblanc and N. Furukawa, Phys. Rev. **B58**, 6414 (1998).
 - [18] A. Moreo, S. Yunoki, and E. Dagotto, Science **283**, 2034 (1999).
 - [19] A. Chattopadhyay, A.J. Millis, and S. Das Sarma, Phys. Rev. **B61**, 10738 (2000).
 - [20] A. Chattopadhyay, A.J. Millis, and S. Das Sarma, Phys. Rev. **B64**, 012416 (2001).

- [21] L. Yin, Phys. Rev. B**68**, 104433 (2003).
- [22] M. Yamanaka, W. Koshibae, and S. Maekawa, Phys. Rev. Lett. **81**, 5604 (1998).
- [23] W. Koshibae, M. Yamanaka, M. Oshikawa, and S. Maekawa, Phys. Rev. Lett. **82**, 2119 (1999).
- [24] R.E. Peierls, *Quantum Theory of Solids*, Clarendon Press, Oxford, 1955.
- [25] E. Müller-Hartmann and E. Dagotto, Phys. Rev. B**54**, R6819 (1996).
- [26] M.J. Calderón and L. Brey, Phys. Rev. B**58**, 3286 (1998).
- [27] Y. Hasegawa, P. Lederer, T.M. Rice, and P.B. Wiegmann, Phys. Rev. Lett. **63**, 907 (1989).
- [28] A. Satou and M. Yamanaka, cond-mat/0001314.
- [29] K. Ohgushi, S. Murakami, and N. Nagaosa, Phys. Rev. B**62**, R6065 (2000).
- [30] D.F. Agterberg and S. Yunoki, Phys. Rev. B**62**, 13816 (2000).
- [31] Y.B. Kim, P. Majumdar, A.J. Millis, and B.I. Shraiman, cond-mat/9803350; J. Ye, Y.B. Kim, A.J. Millis, B.I. Shraiman, P. Majumdar, and Z. Tesanovic, Phys. Rev. Lett. **83**, 3737 (1999).
- [32] M.J. Calderon and L. Brey, Phys. Rev. B**63**, 054421 (2001).
- [33] H. Aliaga, B. Normand, K. Hallberg, M. Avignon, and B. Alascio Phys. Rev. B**64**, 024422 (2001).
- [34] J.L. Alonso, L.A. Fernández, F. Guinea, V. Laliena, and V. Martín-Mayor Phys. Rev. B**63**, 064416 (2001).
- [35] J.L. Alonso, J.A. Capitan, L.A. Fernández, F. Guinea, and V. Martín-Mayor Phys. Rev. B**64**, 054408 (2001).
- [36] M.S. Reis, J.C.C. Freitas, M.T.D. Orlando, E.K. Lenzi, and I.S. Oliveira, Europhys. Lett. **58**, 42 (2002).
- [37] M.S. Reis, V.S. Amaral, J.P. Araújo, and I. S. Oliveira, Phys. Rev. B**68**, 014404 (2003).
- [38] M.S. Reis, J.P. Araújo, V.S. Amaral, E.K. Lenzi, and I.S. Oliveira, Phys. Rev. B**66**, 134417 (2002).
- [39] The “incommensurate” means that the spin configuration is characterized by a k_F incommensurate configuration. The corresponding transfer integral has a $2k_F$ modulation.
- [40] For a review, see H. Kawamura, J. Phys.: Condens. Matter **10** 4707 (1998) and references therein.
- [41] E.M. Kogan and M.I. Auslender, Physica Status Solidi B**147**, 613 (1988).
- [42] A.J. Millis, P.B. Littlewood, and B.I. Shraiman, Phys. Rev. Lett. **74**, 5144 (1995).